Journal of Nuclear Materials 122 & 123 (1984) 1453-1458
North-Holland, Amsterdam

SIMULATION OF PLASMA DISRUPTION INDUCED MELTING AND VAPORIZATION BY ION OR ELECTRON BEAM

Ahmed M. HASSANEIN

Argonne National Laboratory, Fusion Power Program, 9700 South Cass Avenue, Argonne, IL 60439

The exact amount of vaporization losses and melt layer thickness resulting from a plasma disruption are very important to fusion reactor design and lifetime. Experiments using ion or electron beams to simulate the disruption effects have different environments than the actual disruption conditions in fusion reactors. A model has been developed to accurately simulate the beam-target interactions so that the results from such experiments can be meaningful and useful to reactor design. This model includes a two dimensional solution of the heat conduction equation with moving boundaries. It is found that the vaporization and melting of the sample strongly depends on the characteristics of the beam spatial distribution, beam diameter, and on the power-time variation of the beam.

1. INTRODUCTION

Intense energy fluxes on the plasma chamber wall, limiters, or divertor plates, and other components will be encountered in magnetic fusion devices. Of particular concern is the plasma dump following a hard disruption. The energy deposited on part of the first wall during the plasma disruption in fusion devices could exceed 300 MJ and the deposition time is estimated to be between 1 ms and 100 ms. As a result, the energy flux may reach values up to 1000 KW/cm^2 or more. Increasing attention is being given to the possible effects of this intense, short pulse heat loads on materials and the resulting melting and vaporization and the influence of these processes on fusion reactor design and its lifetime. Considerable progress has been made in the theoretical modeling of plasma disruption and the description of the melt layer formation and the vaporization losses expected during a disruption in fusion reactors.[1,2] However, in the past, experimental work to directly simulate disruption melting and vaporization for energy densities and deposition times expected in fusion reactors has been lacking. Recently an Electron Beam Surface Heating Facility (ESURF) has been initiated to study plasma disruption thermal effects.[3] Measurement of melting zone thicknesses and vaporization losses for energy densities up to 1200 J/cm^2 and disruption times varies from 1 ms to 100 ms for different candidate materials is currently underway.[4] Another study uses a pulsed electron beam with 35 keV accelerating voltage to simulate disruption events which focus on the microstructural and chemical changes induced in stainless steel in the vicinity of the threshold for melt layer formation.[5] A third study is planning to use an ion beam to simulate high heat flux and disruption effects on material surfaces.[6]

For these experiments to be meaningful and for the results to be useful to real reactor design, an accurate theoretical simulation of the beam-target interactions is needed. The lacking of such models has forced experimentalists to impose certain conditions on their experiments to avoid effects resulting from lateral heat conduction and beam spatial distribution. Some of these conditions are to use larger beam diameters or smaller samples. Larger beam diameters tend to result in fluctuations in the beam power density which cause instabilities and consequently appreciable lateral motion within the molten layer giving inaccurate estimations of the melting and

0022-3115/84/$03.00

vaporization losses. The purpose of this study is to develop a model to accurately simulate different experimental conditions and beam characteristics. In this model a two dimensional heat conduction equation in cylindrical coordinates with moving boundaries is solved. One moving boundary being the melt-solid interface for each coordinate and another moving boundary is the surface receding as a result of evaporation.

2. FORMULATION OF THE PROBLEM

The time dependent heat conduction equation in axially symmetric cylindrical coordinates (r,z), where r being the radial distance measured from the center of the beam and z being the coordinate normal to the sample surface with origin at the surface (as shown in Fig. 1), is given by

$$\rho c \frac{DT}{Dt} = \frac{1}{r}\frac{\partial}{\partial r}\left(kr \frac{\partial T}{\partial r}\right) + \frac{\partial}{\partial z}\left(k \frac{\partial T}{\partial z}\right) + \dot{q}\ (r,z,t) \quad (1)$$

where ρ = density
c = specific heat
k = thermal conductivity
$T \equiv T\ (r,z,t)$, and
$\dot{q}\ (r,z,t)$ = volumetric energy deposition rate

All the thermophysical properties are assumed to be a function of the local temperature. One boundary condition is that for large distances into the specimen the temperature is assumed to be constant and equal to the ambient sample temperature, T_b, i.e.,

$$T\ (\infty,z,t) = T\ (r,\infty,t) = T_b \quad (2)$$

The surface temperature is determined by both the boundary condition as well as by the evaporation process. The correct boundary condition requires partitioning of the incident energy into conduction, melting, evaporation, and radiation. The kinetics of evaporation establish the connection between the surface temperature and the net atom flux leaving the surface taking into account the possibility of recondensation.[7]

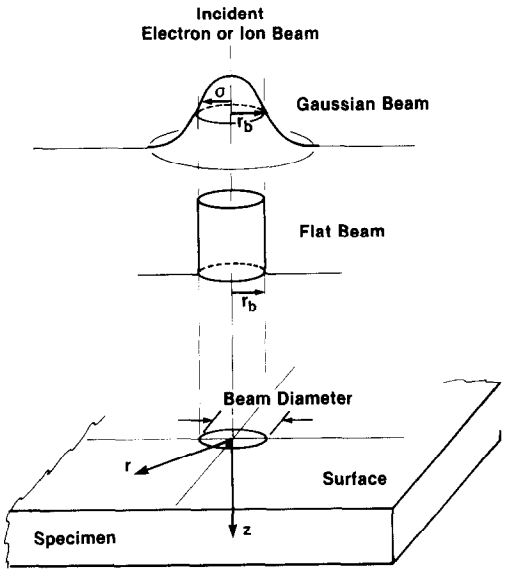

FIGURE 1
Schematic illustrating ion or electron beam - target interaction.

The boundary condition on the surface, for any radial heat flux F(r,t), is then given by

$$F(r,t) = -K\ (T_v) \frac{\partial T}{\partial z} + \rho\ (T_v)\ L_v\ v\ (T_v) + \sigma_s\ \varepsilon\ (T_v^4 - T_o^4) \quad (3)$$

where $T_v = T\ (r,o,t)$, L_v is the material heat of vaporization, and $v\ (T_v)$ is the velocity of the receding surface. This velocity is a function of the instantaneous surface temperature and other material parameters.[1] The radiative heat transfer term contains the Stefan-Boltzmann constant, σ_s, the material emissivity ε, and the temperature T_o of the cold portion of the surroundings to the experiment.

Once melting occurs, the requirement on the continuity of temperature at the solid-liquid

interface $z = m(r,t)$ is given as

$$T_s(r,z,t) = T_\ell(r,z,t) = T_m \tag{4}$$

where $T_s(r,z,t)$ and $T_\ell(r,z,t)$ are the temperatures of the solid and the liquid phases, respectively, and T_m is the melting (or solidification) temperature which is constant for a given material.

The energy equation at the solid-liquid interface, for which the location of this interface is given as $F(r,z,t) = z - m(v,r,t) = 0$, takes the form[8]

$$\left[1 + \left(\frac{\partial m}{\partial r}\right)^2\right]\left[k_s \frac{\partial T_s}{\partial z} - k_\ell \frac{\partial T_\ell}{\partial z}\right] = \rho L_f \frac{\partial m}{\partial t} \tag{5}$$

where L_f is the latent heat of fusion.

If the heating is continued long enough and at a sufficiently high rate, significant vaporization will occur from the surface assuming the melting material stays in place. It is necessary to account for the receding surface at the interface between vapor and solid or liquid. This can be done by introducing a moving coordinate system in which the instantaneous surface $z(r,t)$ is defined as

$$z(r,t) = z_0 - {}_0\int^t v(r,t)\, dt \tag{6}$$

where $z_0 = 0$ is the original surface.

Transforming the heat conduction equation (1) to this moving coordinate, the total time derivative is then given by

$$\frac{DT}{Dt} = \frac{\partial T}{\partial t} + \frac{\partial T}{\partial z}\frac{dz}{dt} = \frac{\partial T}{\partial t} - v(r,t)\frac{\partial T}{\partial z} \tag{7}$$

Then the modified heat conduction equation is given by

$$\rho c \frac{\partial T}{\partial t} = \frac{1}{r}\frac{\partial}{\partial r}\left(Kr \frac{\partial T}{\partial r}\right) + \frac{\partial}{\partial z}\left(K \frac{\partial T}{\partial z}\right) + \rho c\, v(r,t) \frac{\partial T}{\partial z} + \dot{q}(r,z,t) \tag{8}$$

which includes the additional convective term $\rho c v(r,t) \frac{\partial T}{\partial z}$ that can be important in the cases of intensive evaporation if we are to obtain accurate calculations of the temperature.

The velocity of the receding surface, i.e., $v(r,t)$ is a highly non-linear function of temperature. A review of the model used to calculate the evaporation losses is given in reference 7. In this model, the surface velocity is given by

$$v(r,t) = 5.8 \times 10^{-2} \frac{\alpha \sqrt{A}\, P_v(T_v)}{\rho(T_v)\sqrt{T_v}} \left[0.8 + 0.2\, e^{-t/10\tau_c}\right] \quad \text{cm/sec} \tag{9}$$

where α = sticking probability (usually = 1)
A = atomic mass number of target material
P_v = vapor pressure (Torr)
τ_c = vapor collision frequency (sec^{-1})

The total mass loss due to evaporation can then be given by

$$\Delta m = \int_{t=0}^{t_\infty} \int_{r=0}^{r_\infty} 2\pi\, r \rho v(r,t)\, dr\, dt \tag{10}$$

where t_∞ and r_∞ are the time and the distance at which the temperature drops to a low value such that no significant vaporization losses take place.

3. RESULTS FROM DISRUPTION SIMULATION

A computer code A*THERMAL-2 has been developed to solve the two dimensional heat conduction equation with moving boundaries by finite difference techniques. The description of the code and the numerical methods used in the solution will be published elsewhere.

The calculation is performed parametrically assuming a radially symmetric stationary beam with different diameters and with either Gaussian or flat energy density distribution. The calculations presented here assume a beam energy

density of 800 J/cm^2 (corresponding to a flat beam) deposited in 50 ms or 20 ms on copper and stainless steel with an initial sample temperature of 300°C. These conditions are chosen from actual disruption tests currently being conducted at ESURF on a number of candidate materials.[4] The total beam energy for a flat beam is simply the energy density multiplied by the area of the beam. For the Gaussian distribution the surface heat flux F(r) is given by

$$F(r) = F_0 \, e^{-r^2/2\sigma^2} \tag{11}$$

where F_0 is the maximum heat flux at the center of the beam. The standard deviation σ can be calculated by noting that at $r = r_b$ (the nominal beam spot radius), the local heat flux is one half of the maximum. This gives

$$\sigma^2 = 0.72 \, r_b^2 \tag{12}$$

The total beam power P_t, in a Gaussian profile, is given by

$$P_t = 2\pi F_0 \int_0^\infty e^{-r^2/2\sigma^2} \, r dr = 2\pi\sigma^2 F_0 \tag{13}$$

Note that integrating Equation (13) from r = 0 to r = 3σ yields more than 98% of the total beam energy. The maximum heat flux at the center of the Gaussian beam i.e., F_0 is given from Equation (13) by equating the total energy with that for the flat beam. It is obvious that this maximum heat flux is less than that of a flat beam with the same total energy. However, we are comparing two different beam profiles containing the same total energy which, from an experimental point of view, is more precisely known than the profile.

The maximum surface temperature rise (i.e., at the center of the beam) is shown in Figure 2 for both copper and stainless steel for an energy density of 800 J/cm^2 deposited in 50 ms. The copper surface temperature rise is shown for different flat beam diameters. The temperature starts rising after starting beam deposition and it reaches its maximum at the end of the deposition time, then it decreases sharply. For beam diameters greater or equal to 1 mm, the surface temperature for stainless steel is much higher than that for copper and the temperature stays in the liquid phase for about 100 ms. For beam diameters greater or equal to 3 mm, the copper melts for a duration of about 35 ms. Lateral conduction along the beam surface becomes very important for smaller beam diameters as it can be seen that for a beam diameter of 1 mm under the same condition copper shown does not even melt.

Figure 3 shows the maximum melting zone thickness and the maximum vaporization losses (i.e., at r = 0) as a function of the beam diameter for both copper and stainless steel. Copper shows very little vaporization at the condition shown and only for beam diameters larger than 2 mm, while melting occurs for beam diameters equal or larger than 1.2 mm. Substantial effects from different beam diameters can result from different beam spatial distribution profiles and from longer deposition times.

The spatial variation of the melting zone thickness along the beam radial distance is shown for copper in Figure 4 for different flat beam diameters. The maximum melting thickness at the center of the beam strongly depends on the beam diameter up to 4 mm for the conditions shown. The melting width in the radial direction also depends on the beam diameter and for copper it is always less than the beam diameter. The larger the diameter of the beam the closer the melting zone width to the beam diameter. For stainless steel and flat beam diameter larger than 1 mm, it is found that the melting width in the radial direction is always larger than the beam diameter.

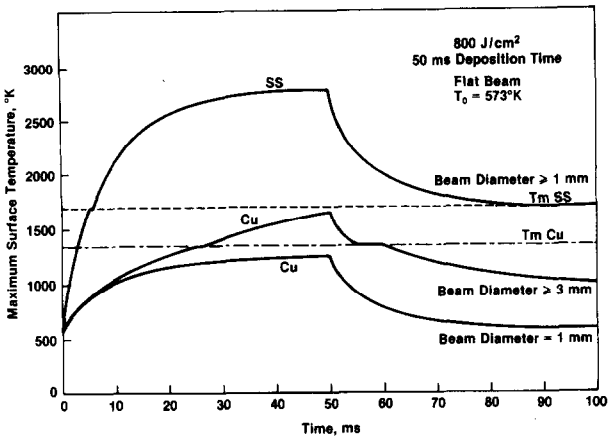

FIGURE 2
Surface temperature rise at the center of the beam for copper and stainless steel.

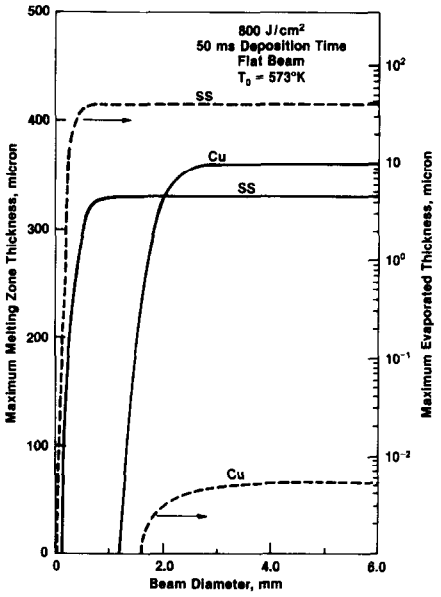

FIGURE 3
Maximum melting zone and vaporization losses as a function of flat beam diameter.

For a Gaussian beam with the same total energy, it is found that copper, under the same conditions, does not melt even for beam diameters as large as 10 mm.[9]

The radial distribution of the vaporized stainless steel material is shown in Figure 5 for flat and Gaussian beam distributions. Two cases are considered for the same average energy density. The first case is for a beam diameter

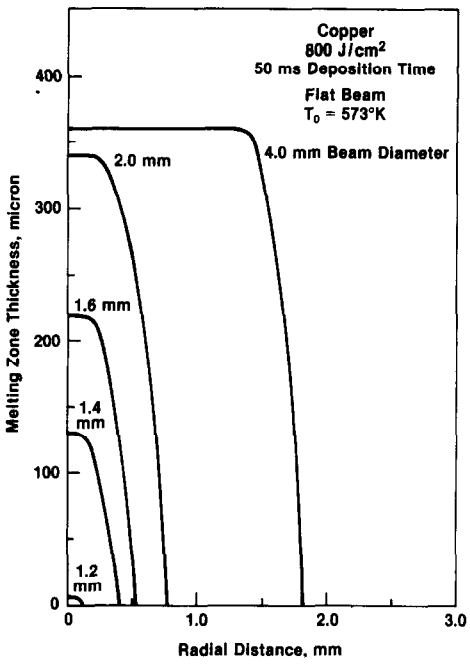

FIGURE 4
Copper melting zone width and thickness for different beam diameters.

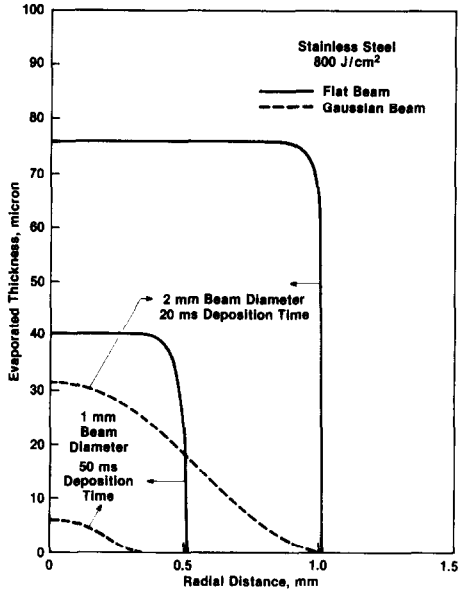

FIGURE 5
Stainless steel vaporization losses for different beam distribution and different deposition time.

of 1 mm and 50 ms deposition time, and the second case is for 2 mm beam diameter and 20 ms deposition time. It can be seen that the flat beam results in a much more total material loss than that from the Gaussian beam and the difference is larger for longer deposition times (for the same beam total energy).

Another important factor of the beam transient characteristics is the time shape of the loading pulse. It is found that, for example, a triangular time pulse with the same total energy produces more evaporation and less melting than the square time pulse used in this calculation.[9] Also higher sample initial temperatures can be used to reduce threshold beam energy needed to induce melting and cause significant vaporization.[9]

4. CONCLUSIONS

A model has been developed to accurately simulate the interaction of high power electron, ion, or laser beams with material. This model includes a two dimensional solution of the heat conduction equation with phase change and moving boundaries. The model has been applied to study melting and vaporization of stainless steel and copper resulting from an electron beam energy deposition. The conclusions reached from this study are:

(1) The transient characteristics of the electron or ion beam can have significant effect on the thermal behavior at the surface of the material.

(2) There is a minimum beam diameter below which lateral heat conduction is very important and strongly affects melting and vaporization at the center of the beam. This beam diameter depends on the kind of material as well as on the time and shape of the energy deposited.

(3) The maximum and the total amount of material melted and vaporized are strongly dependent on the beam distribution profile for the same total beam energy.

(4) The shape of the power density variation in time can substantially affect the melting and vaporization losses of the material.

(5) Higher initial material temperatures can be used to reduce the required beam energy to induce melting and vaporization.

ACKNOWLEDGEMENT

This work has been supported by the U.S. Department of Energy.

REFERENCES

1. A. M. Hassanein, G. L. Kulcinski, and W. G. Wolfer, J. Nucl. Mat. 103/104 (1981) 321.

2. B. Merrill, Contribution to US INTOR Report INTOR/NUC/81-7, June, 1981

3. J. W. H. Chi, Transient surface phenomena from electron beam surface heating tests conducted in ESURF, Westinghouse Advanced Reactors Division, FE-TN-82-6, November, 1982.

4. J. R. Easoz, private communication.

5. S. T. Picraux, T. A. Knapp, M. J. Davis, to be published in J. Nucl. Mat.

6. High Heat Flux Group, Sandia National Laboratory.

7. A. M. Hassanein, G. L. Kulcinski, and W. G. Wolfer, to be published in Nuclear Eng. and Design/Fusion.

8. M. N. Ozisik, Heat Conduction, Wiley-Interscience, New York (1980).

9. A. M. Hassanein, Modeling the interaction of high power ion or electron beams with solid materials, ANL/FPP/TM-179, (Nov. 1983).